AD_____

Award Number: DAMD17-00-1-0170

TITLE: Are Microtubules Involved in Anoikis?

PRINCIPAL INVESTIGATOR: Steven M. Frisch, Ph.D.

CONTRACTING ORGANIZATION: The Burnham Institute
La Jolla, California 92037

REPORT DATE: August 2003

TYPE OF REPORT: Final

PREPARED FOR: U.S. Army Medical Research and Materiel Command
Fort Detrick, Maryland 21702-5012

DISTRIBUTION STATEMENT: Approved for Public Release;
Distribution Unlimited

The views, opinions and/or findings contained in this report are those of the author(s) and should not be construed as an official Department of the Army position, policy or decision unless so designated by other documentation.

20040503 035

REPORT DOCUMENTATION PAGE

Form Approved
OMB No. 074-0188

Public reporting burden for this collection of information is estimated to average 1 hour per response, including the time for reviewing instructions, searching existing data sources, gathering and maintaining the data needed, and completing and reviewing this collection of information. Send comments regarding this burden estimate or any other aspect of this collection of information, including suggestions for reducing this burden to Washington Headquarters Services, Directorate for Information Operations and Reports, 1215 Jefferson Davis Highway, Suite 1204, Arlington, VA 22202-4302, and to the Office of Management and Budget, Paperwork Reduction Project (0704-0188), Washington, DC 20503

1. AGENCY USE ONLY (Leave blank)	2. REPORT DATE	3. REPORT TYPE AND DATES COVERED
	August 2003	Final (1 Aug 2000 - 31 Jul 2003)

4. TITLE AND SUBTITLE
Are Microtubules Involved in Anoikis?

5. FUNDING NUMBERS
DAMD17-00-1-0170

6. AUTHOR(S)
Steven M. Frisch, Ph.D.

7. PERFORMING ORGANIZATION NAME(S) AND ADDRESS(ES)
The Burnham Institute
La Jolla, California 92037

E-Mail: sfrisch@burnham.org

8. PERFORMING ORGANIZATION REPORT NUMBER

9. SPONSORING / MONITORING AGENCY NAME(S) AND ADDRESS(ES)
U.S. Army Medical Research and Materiel Command
Fort Detrick, Maryland 21702-5012

10. SPONSORING / MONITORING AGENCY REPORT NUMBER

11. SUPPLEMENTARY NOTES
Original contains color plates: All DTIC reproductions will be in black and white.

12a. DISTRIBUTION / AVAILABILITY STATEMENT
Approved for Public Release; Distribution Unlimited

12b. DISTRIBUTION CODE

13. ABSTRACT (Maximum 200 Words)

This project is investigating the role of microtubule alterations in anoikis, with a view toward re-examining the mechanism of microtubule-targeting drugs such as taxol.

During the past year, we have uncovered a new mechanism by which cell adhesion controls apoptosis. The death receptor adaptor protein FADD (FAS-associated death domain protein) is critical for anoikis as well as death ligand (e.g., FASL)- induced apoptosis. Recently, we discovered that FADD is primarily in the nucleus of attached cells, where it is unavailable for apoptosisi induction. Detachment of mammary epithelial cells form extracellular matrix, however, provokes the export of FADD form the nucleus, thus promoting apoptosis.

Our preliminary work suggests that microtubule drugs can promote FADD export, suggesting a new mechanism by which the can promote apoptosis. This is expected to have major ramifications for optimizing the use of taxol or other microtubule drugs in connection with other agents that may promote apoptosis.

During the latter year of the project, we found that a protein kinase known as Glycogen Synthase Kinase-3 (GSK-3) phosphorylates FADD and that this phosphorylation is required for both the transport of FADD into and out of the nucleus. In that GSD-3 is a microtubule-regulatory kinase, this represents a new link between microtubules and apoptosis.

14. SUBJECT TERMS
Microtubules, FADD, Nuclear export, apoptosis

15. NUMBER OF PAGES
23

16. PRICE CODE

17. SECURITY CLASSIFICATION OF REPORT	18. SECURITY CLASSIFICATION OF THIS PAGE	19. SECURITY CLASSIFICATION OF ABSTRACT	20. LIMITATION OF ABSTRACT
Unclassified	Unclassified	Unclassified	Unlimited

Table of Contents

Cover	**1**
SF 298	**2**
Table of Contents	**3**
Introduction	**4**
Body	**4**
Key Research Accomplishments	**6**
Reportable Outcomes	**6**
Conclusions	**7**
References	**7**
Appendices	**7**

INTRODUCTION

Anoikis, defined as apoptosis that is inhibited by extracellular matrix[1], plays a major role in mammary gland development and in safeguarding against breast cancer metastasis. [1,2] While most studies on anoikis have focused on the role of integrin signaling through the actin cytoskeleton[1], the potential role of the microtubule component has been overlooked – despite the fact that microtubules are the targets of major breast cancer drugs such as taxol. The original goals of this project were to determine the role of microtubules in anoikis, using two approaches: i. by determining the effect of cell adhesion upon microtubules and ii. by determining the effect of microtubule alterations on integrin signaling pathways. However, in the course of this study, we fortuitously discovered a novel and unexpected property of mammary epithelial cells that is likely to shed major new insight into the microtubule-apoptosis connection (see below).

BODY

In the course of investigating the role of FAS-Associated Death Domain protein (FADD) in anoikis, we discovered that it is primarily a nuclear protein. It interacts with a DNA repair enzyme and may mechanistically translate DNA damage signals into apoptosis signaling through FADD-caspase-8 complexes (see reportable outcome #1 below). We therefore investigated caspase-8, the direct effector protein for FADD. Indeed, some caspase-8 was nuclear as well (data not shown), but most of the caspase-8 of mammary epithelial cells (MCF10a) was in centrosomes (figure 1).

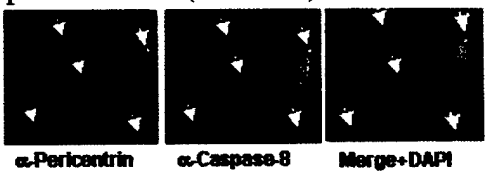

Figure 1. MCF10a cells were fixed with cold methanol and stained with anti-pericentrin pAb (Covance) plus anti-caspase-8 mAb antibody (Pharmingen) followed by detection with anti-rabbit-Alexa 488 and anti-mouse-Alexa-594.

Centrosomes are known to become unstable in human tumor cells[3], including breast cancer [4,] where they become supernumerary (i.e., more than 2 in mitotic cells). This is thought to contribute to both chromosomal instability and the loss of epithelial cell polarity in tumor cells[3-6]. It was therefore of great interest to determine whether caspase-8 – which is known to be involved in apoptosis control including anoikis[7] – might also be linked to centrosome function.

To test this, we expressed the specific caspase-8 inhibitor crmA in MCF10a and MDCK cells and monitored centrosomes. Indeed, crmA caused the rapid appearance of multiple centriolar structures (figure 2,3). This occurred even in transiently transfected cells (figure 2) ruling out the possibility that inhibition of caspase-8 relieved a selection against aberrant cells. Also, FADD-knockout cells and bcl-2-overexpressing MDCK cells – both of which were highly apoptosis-resistant – did not show an elevated rate of abnormal centrosomes, further arguing that relief of apoptosis was not the major mechanism for the crmA effect.

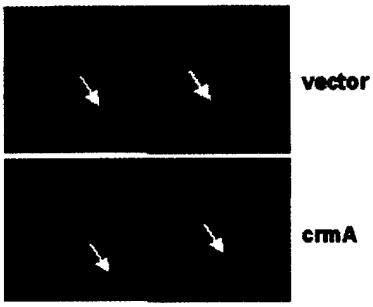

Figure 2. Inhibition of caspase-8 using crmA induces centrosome hypertrophy. MCF10a cells were transiently transfected with EYFP-centrin (a centriolar protein) together with a crmA expression plasmid or an empty vector. Cells were fixed 36 hours post-transfection and photographed. Two representative cells are shown for each sample; similar centrosome anomalies were detected in about 50% of the cells with crmA and were undetectable in the vector-transfected cells.

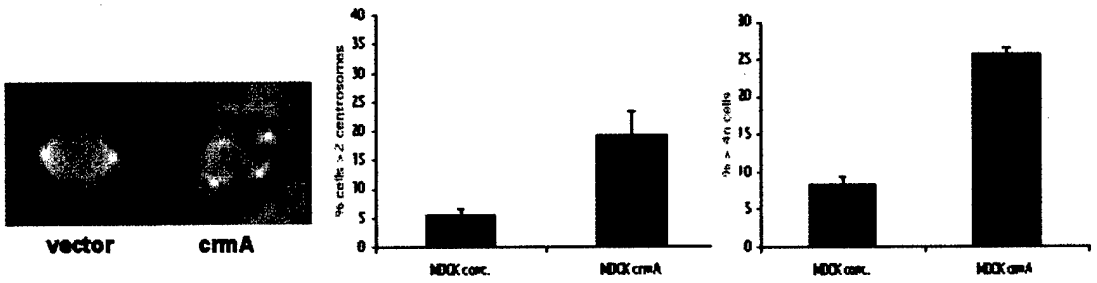

Figure 3. Inhibition of caspase-8 using crmA induces centrosome hypertrophy, aberrant mitoses and polyploidy in MDCK cells. Stable crmA –expressing MDCK cells were stained for pericentrin (yellow), β–tubulin (green) and chromatin (blue); representative cells are shown. Frequencies of cells with supernumerary centrosomes (middle) and polyploidy (right; as determined by flow cytometry of propidium iodide-stained cells) are shown.

To demonstrate more definitively that caspase-8 was involved in centrosome function, we compared caspase-8-null mouse embryo fibroblasts (MEFs) vs. control MEFs. The caspase-8 knockout cells clearly had a higher frequency of aberrant centrosomes and, consequently, aberrant mitotic spindles (figure 3).

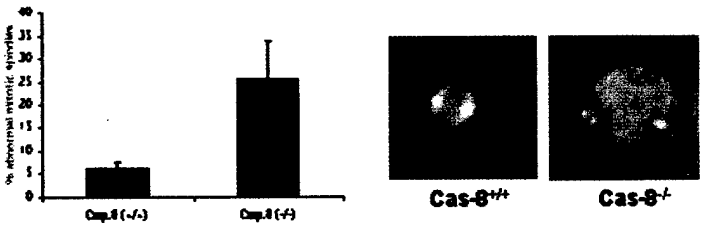

Figure 3. Caspase-8-null and caspase-8-wild-type MEFs (from David Wallach, Weizmann Institute) were stained with anti-pericentrin (red-yellow), anti-β–tubulin

(green) and DAPI. The frequency of aberrant mitotic spindles was calculated and shown in the graph.

To determine whether the capase-8 catalytic activity might be required for normal centrosome function, we inhibited all cellular caspase activity for 24 hours in EYFP-centrin-transfected cells. Indeed, treated cells showed an elevated number of centrioles, suggesting that caspase activity (presumably caspase-8) is required for some aspect of centriole duplication/maturation (figure 4).

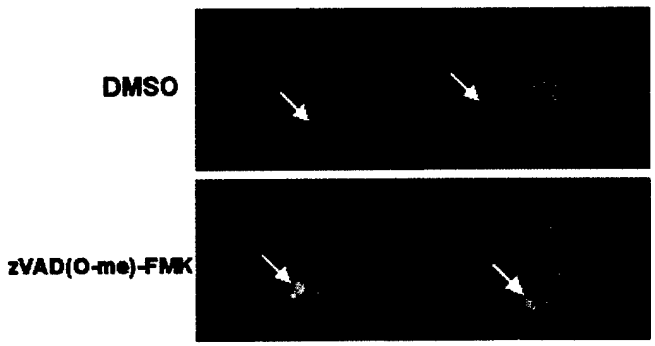

Figure 4. MCF10a cells (asynchronously growing) that had been transfected with EYFP-centrin were treated with 25 μM z-VAD(O-me)-FMK or the same volume of DMSO for 24 hours prior to photography. Representative cells are shown.

As mentioned above, centrosomes (the microtubule organizing centers of the cell) are critical for epithelial polarity and chromosomal stability, two phenotypic features which are dysregulated in breast cancer cells. These data suggest that caspase-8 may be involved in normal centrosomal regulation, and motivate a search for caspase-8 deficiency in breast cancer cells, as has been demonstrated in certain other tumor types[8]. More generally, these data suggest that inhibition of caspase pathways may directly cause centrosomal instability and its harmful consequences for tumor progression.

KEY RESEARCH ACCOMPLISHMENTS

-- The microtubule organizing center of the cell, the centrosome, is the site of caspase-8 localization in mammary epithelial cells.
--Inhibition of caspase-8 expression or catalytic activity disrupts the centrosome cycle.

REPORTABLE OUTCOMES

Screaton RA, Kiessling S, Sansom OJ, Millar CB, Maddison K, Bird A, Clarke AR, and Frisch SM. Fas-associated death domain protein interacts with methyl-CpG binding domain protein 4: a potential link between genome surveillance and apoptosis. *Proc. Natl. Acad. Sci.* 100: 5211-5216, 2003.

Finlay, D., Linke, S., Shah, V. and Frisch, S.M. Caspase-8 is essential for the centrosome cycle. (manuscript in preparation).

CONCLUSIONS

--Caspase-8 has a novel function in centrosome duplication/maturation;

--Tumor cells that lack caspase-8 that fail to activate it properly - due to inhibitory proteins or absence of activating proteins – are prone to centrosomal instability and its consequences: chromosomal instability and loss of epithelial polarity, which contribute to tumor progression.

REFERENCES

1. Frisch SM, Screaton RA. Anoikis Mechanisms Curr. Opin. Cell Biol. (2001) 13: 555-562.

2. Streuli C., Gilmore A. Adhesion-mediated signaling in the regulation of mammary epithelial cell survival. (1999) J. Mammary Gland Biol Neoplasia 4:183-191

3. Doxsey, S. Re-evaluating centrosome function. Nature Rev. Molec. Cell Biol. 2: 688-698, 2001

4. Lingle, W., Lutz, W., Ingle, J., Maihle, N., and Salisbury, J. Centrosome hypertrophy in human breast tumors: implications for genomic stability and cell polarity. Proc. Natl. Acad. Sci. 95: 2950-2955, 1998.

5. Nigg, E. Centrosome aberrations: cause or consequence of cancer progression? Nature Rev. Cancer 2: 1-6, 2002

6. Etienne-Manneville, S. and Hall, A. Cdc42 regulates GSK-3 and APC to control cell polarity. Nature 421: 753-756, 2003

7. Rytomaa M, Martins LM, Downward J. Involvement of FADD and caspase-8 signalling in detachment-induced apoptosis. Oncogene. 19:4461-8, 2000

8. Teitz, T., Wei, T., Valentine, M. B., Vanin, E. F., Grenet, J., Valentine, V. A., Behm, F. G., Look, A. T., Lahti, J. M., and Kidd, V. J., Caspase 8 is deleted or silenced preferentially in childhood neuroblastomas with amplification of MYCN. *Nature Medicine, 6*, 529 (2000).

APPENDIX

Screaton RA, Kiessling S, Sansom OJ, Millar CB, Maddison K, Bird A, Clarke AR, and Frisch SM. Fas-associated death domain protein interacts with methyl-CpG binding domain protein 4: a potential link between genome surveillance and apoptosis. *Proc. Natl. Acad. Sci.* 100: 5211-5216, 2003.

Fas-associated death domain protein interacts with methyl-CpG binding domain protein 4: A potential link between genome surveillance and apoptosis

Robert A. Screaton*, Stephan Kiessling*, Owen J. Sansom†, Catherine B. Millar‡, Kathryn Maddison†, Adrian Bird‡, Alan R. Clarke†, and Steven M. Frisch*§

*The Burnham Institute, 10901 North Torrey Pines Road, La Jolla, CA 92037; †Cardiff School of Biosciences, Cardiff University, P.O. Box 911, Cardiff CF10 3US, United Kingdom; and ‡Wellcome Trust Centre for Cell Biology, The King's Buildings, Edinburgh University, Edinburgh EH9 3JR, United Kingdom

Communicated by Erkki Ruoslahti, The Burnham Institute, La Jolla, CA, February 28, 2003 (received for review January 22, 2003)

Fas-associated death domain protein (FADD) is an adaptor protein bridging death receptors with initiator caspases. Thus, its function and localization are assumed to be cytoplasmic, although the localization of endogenous FADD has not been reported. Surprisingly, the data presented here demonstrate that FADD is mainly nuclear in several adherent cell lines. Its accumulation in the nucleus and export to the cytoplasm required the phosphorylation site Ser-194, which was also required for its interaction with the nucleocytoplasmic shuttling protein exportin-5. Within the nucleus, FADD interacted with the methyl-CpG binding domain protein 4 (MBD4), which excises thymine from GT mismatches in methylated regions of chromatin. The MBD4-interacting mismatch repair factor MLH1 was also found in a complex with FADD. The FADD–MBD4 interaction involved the death effector domain of FADD and a region of MBD4 adjacent to the glycosylase domain. The FADD-binding region of MBD4 was downstream of a frameshift mutation that occurs in a significant fraction of human colorectal carcinomas. Consistent with the idea that MBD4 can signal to an apoptotic effector, MBD4 regulated DNA damage-, Fas ligand-, and cell detachment-induced apoptosis. The nuclear localization of FADD and its interaction with a genome surveillance/DNA repair protein that can regulate apoptosis suggests a novel function of FADD distinct from direct participation in death receptor signaling complexes.

DNA damage-induced apoptosis signals originate in the nucleus. For example, double-strand DNA breaks activate the ATM/ATR (1) and c-abl-related kinases (2), leading to activation of the p53-family proteins (3, 4) and subsequent apoptosis. Other forms of DNA damage that are repaired by the mismatch repair (MMR) complex (reviewed in refs. 5 and 6) can promote apoptosis through the MMR component MLH1. Thus, MLH1 defects in tumor cells cause apoptosis resistance with regard to several DNA-damaging drugs (7–11). In fact, all five major types of DNA repair complexes are thought to signal to the apoptotic machinery (reviewed in ref. 12), although the mechanism of signaling is largely unknown.

Interestingly, several apoptosis-regulatory proteins are in the nucleus constitutively or conditionally. These include PEA-15 (13), DEDD 1–3 (14–16), DEDAF (17), p84N5 (18), caspases-2 (19) and -6 (20), Daxx (21), and (under conditions where nuclear export is inhibited) TRADD (22). Possible roles for these proteins in nuclear apoptotic signaling remain to be determined.

Recently, we have identified an additional link between a DNA repair protein and apoptosis (O.J.S. and A.R.C., unpublished data), namely the protein methyl-CpG binding domain protein 4 [MBD4 (23), also known as MED1 (24)]: MBD4 promoted the apoptotic response to DNA-damaging agents. The N-terminal conserved MBD of this protein targets it to bind methylated regions of DNA, whereas the C terminus is a uracil/thymine-*N*-glycosylase. The latter excises spontaneously deaminated cytosine (i.e., uracil) or methylcytosine (i.e., thymine) from G-T/U mismatches (25–27), the major individual source of point mutations in the human genome (28). MBD4 interacts with the mismatch repair/tumor suppressor protein MLH1 (24); both are mutator genes (29, 30). The inactivation of either gene causes increased apoptosis resistance with regard to DNA-damaging agents (refs. 7–11; O.J.S. and A.R.C., unpublished data), implying possible apoptotic signaling functions for both proteins. As with MLH1 (reviewed in ref. 30), MBD4 and also frequently mutated in certain human tumors (6, 31–34). The mechanistic link between MBD4, MLH1, and apoptosis will be important to elucidate.

Fas-associated death domain protein (FADD) is known mainly for its death receptor adaptor function at the cell surface (35–37). Thus, it is widely assumed that FADD is primarily or solely a cytoplasmic protein. However, there are no published data clearly supporting this assumption (see *Discussion*). Indeed, FADD has been implicated in potentially death receptor-independent apoptotic responses such as DNA damage and anoikis (38–42) that would not necessarily require FADD to be cytoplasmic. Moreover, cell-matrix adhesion can protect against Fas ligand (FasL)-induced apoptosis (R.A.S. and S.M.F., unpublished observations; refs. 43 and 44), suggesting that certain Fas-interacting proteins might be subject to relocalization by extracellular signals. We therefore examined the subcellular localization of FADD in the hope of revealing additional functions of the protein. Here, we report that FADD primarily localized to the nucleus, implying that the nuclear-cytoplasmic transport of FADD must be actively regulated and that FADD may have a novel nuclear function. We report that exportin-5 is a candidate nucleocytoplasmic transport protein for FADD and that a genome surveillance protein, MBD4, interacts directly with FADD and modulates apoptosis, suggesting a novel link between genome surveillance and apoptosis.

CELL BIOLOGY

Materials and Methods

Cell Lines, Cell Culture, and Transfections. The normal human mammary epithelial cell line MCF10a was used for most experiments in this article. *MBD4−/−* mouse embryo fibroblasts (MEFs) have been described (29). Cells were transfected by using lipofection or infected with retroviruses based on MSCV-ires-zeo (45), and expression of transgenes was checked by Western blotting.

Apoptosis Assays (Cell Culture Experiments). Cells were maintained in low-attachment wells for the indicated times (for anoikis); some cell samples were exposed to recombinant FasL in the presence of enhancer antibody (for FasL). Cell lysates were

Abbreviations: MBD4, methyl-CpG binding domain protein 4; FADD, Fas-associated death domain protein; FasL, Fas ligand; YFP, yellow fluorescent protein; HA, hemagglutinin; NLS, nuclear localization signal; MEF, mouse embryo fibroblast; DED, death effector domain.

§To whom correspondence should be addressed. E-mail: sfrisch@burnham.org.

prepared and assayed fluorimetrically for Ac-DEVD-AFC cleavage activity.

Apoptosis Assays (*in Vivo* Experiments). *MBD4+/+* or *MBD4−/−* mice were injected with the Fas-agonistic antibody Jo-2. Histological sections of the indicated tissues were stained with hematoxylin/eosin and analyzed for apoptosis as described (46).

Antibodies. Most antibodies were obtained from commercial sources; additional FADD polyclonal antibodies were prepared against bacterially produced GST-FADD protein, and a sheep anti-MBD4 was prepared against the C-terminal 180 aa of recombinant MBD4 protein. A detailed characterization of antibodies is presented in Fig. 5, which is published as supporting information on the PNAS web site, www.pnas.org.

Nuclear-Cytoplasmic Fractionation. Nuclear-cytoplasmic fractionation was accomplished by homogenization of cells in hypotonic buffer followed by low-speed (800 × *g*) centrifugation.

Indirect Immunofluorescence. Indirect immunofluorescence was performed on formaldehyde-fixed, Triton X-100-permeabilized cells by using fluorescently tagged secondary antibodies.

Short-Interfering RNA. Short-interfering RNA was introduced by using lipofection of commercially synthesized RNA duplexes.

FADD Export Assay. WT or mutant forms of FADD were expressed with N-terminal yellow fluorescent protein (YFP) tags and C-terminal nuclear localization signals (NLSs) derived from simian virus 40 virus. After transfection, cells were detached for 15 min before formaldehyde fixation and cells were scored for nuclear vs. cytoplasmic localization on a fluorescence microscope.

Cell Surface Fas Coimmunoprecipitation/Western Blotting. Cell surface Fas coimmunoprecipitation/Western blotting was performed by incubating cell cultures with the Fas-agonistic antibody 2R2 (Roche Molecular Biochemicals) followed by cell lysis in Triton X-100-containing buffer, precipitation with protein A-Sepharose, and Western blot analysis.

Yeast Two-Hybrid Screening, Protein Interactions *in Vitro*, Western Blotting, and Immunoprecipitation. Yeast two-hybrid screening, protein interactions *in vitro*, Western blotting, and immunoprecipitation were performed by using standard methodology as described in *Supporting Methods*, which is published as supporting information on the PNAS web site.

See *Supporting Methods* for detailed materials and methods.

Results

FADD Localizes to the Nucleus in Several Cell Lines. In the course of examining the basis for protection against FasL-induced apoptosis by cell adhesion (R.A.S. and S.M.F., unpublished work), we observed that FADD was predominantly nuclear by using a mAb (Fig. 1). Nuclear FADD staining was blocked by preincubation of the antibody with recombinant antigen. We then generated two monospecific anti-human FADD polyclonal antibodies, which confirmed that FADD was primarily nuclear (Fig. 1). FADD was also primarily nuclear in several cell lines (HT1080 fibrosarcoma, Caco-2 colorectal carcinoma, HaCat keratinocytes, human umbilical vein endothelial cells) representative of diverse attached cell types (data not shown); lymphocytes were not examined in this study. This staining pattern was not seen with antibodies against another death receptor adaptor protein TRADD (data not shown) in the absence of leptomycin, in agreement with a previous report (22). It was unlikely that fixation and permeabilization selectively leached a non-nuclear

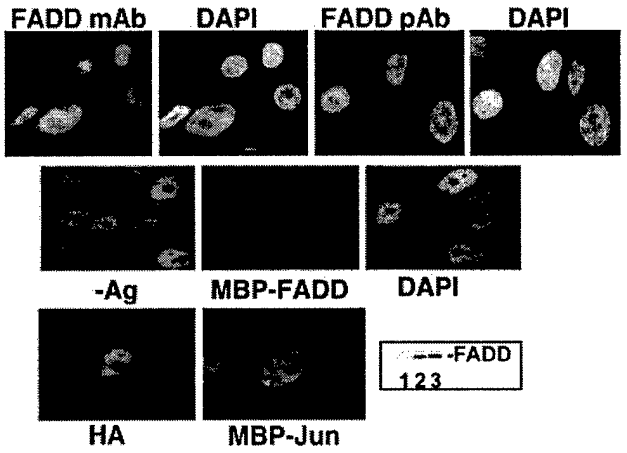

Fig. 1. FADD localizes primarily to the nucleus. (*Top*) MCF10a cells were analyzed for FADD localization by immunofluorescence using a mAb and a polyclonal antibody (pAb); a second pAb produced similar results (data not shown). Nuclear location is indicated by 4′,6-diamidino-2-phenylindole (DAPI) staining. (*Middle*) Immunofluorescent staining was carried out after incubation of the primary antibody (mAb) with recombinant maltose-binding protein fusion proteins of FADD or c-jun. (*Bottom*) MCF10a cells were infected with a retrovirus containing HA-tagged FADD and stained with anti-HA antibody. (*Inset*) Fixation/permeabilization did not extract a detectable pool of FADD. After fixation (lane 2) or fixation plus permeabilization (lane 3) the insoluble fraction was dissolved in SDS sample buffer and analyzed for FADD by Western blotting. Lane 1 contains the soluble fraction from fixation plus permeabilization.

FADD population, because no FADD was found by immunoblotting of the extracted material obtained during these procedures (Fig. 1). Treatment of MCF10a cells with FADD short-interfering RNA reduced both the FADD signal on a Western blot and the average signal intensity of nuclear immunofluorescence (Fig. 6*a*, which is published as supporting information on the PNAS web site). To confirm the specificity of the nuclear signal, we also generated a monospecific anti-mouse FADD antibody and compared the immunofluorescence micrographs by using FADD-knockout MEFs versus FADD-expressing cells (47). The nuclear FADD signal obtained with an anti-mouse FADD polyclonal antibody was reduced to background levels in FADD-knockout MEFs (Fig. 6*a*). Also, certain mutants of FADD (described below) were found in the cytoplasm under the same fixation conditions, further excluding the possibility of a "fixation artifact."

We then tested whether FADD was nuclear by a cell fractionation approach. Hypotonic lysates were subjected to low-speed (800 *g*) centrifugation, yielding a pellet that was highly enriched for nuclei. Equal cell equivalents of nuclear and cytoplasmic fractions were assayed for FADD content by Western blotting (Fig. 6*b*), indicating that the majority of FADD protein was in the nuclear fraction, as was the majority of c-jun protein. By contrast, the cytoplasmic protein procaspase-3 was mainly in the cytoplasmic fraction. It is not yet clear whether the small percentage of FADD found in the cytoplasmic fraction in some experiments was caused by leakage from the nucleus during the extraction procedure, the extent of which varies widely among nuclear proteins (48, 49), or represented a minor cytoplasmic pool that escaped immunofluorescent detection.

Taken together, the data strongly indicated that the primary localization of FADD is in the cell nucleus of adherent cell lines.

Exportin-5 Is a Potential FADD-Shuttling Protein. FADD functions at the membrane as a death receptor adaptor protein, implying that either a minor cytoplasmic pool is maintained constitutively or

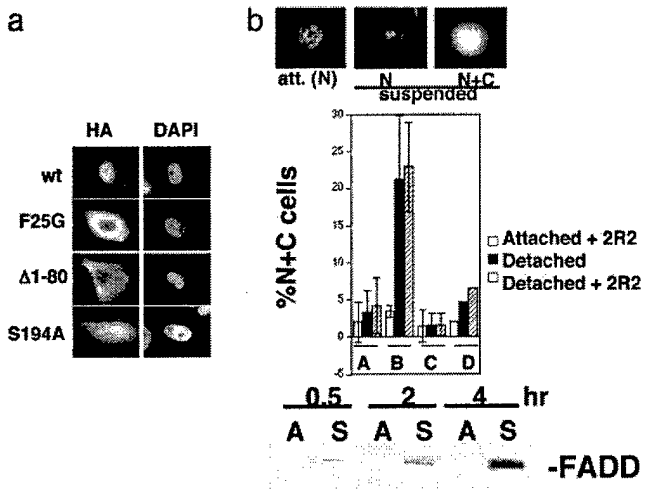

Fig. 2. Characterization of FADD nuclear import/export. (a) Mutation of the Ser-194 phosphorylation site or of the DED (amino acids 1–80) of FADD increases its cytoplasmic accumulation. HA–FADD expression constructs containing the indicated FADD mutants were transfected into MCF10a cells, which were then immunostained with anti-HA antibody after being maintained in attached conditions. Representative HA-stained cells and the positions of their nuclei (4′,6-diamidino-2-phenylindole, DAPI) are shown. (*b*) The same mutations of FADD that cause cytoplasmic accumulation also prevent induction of export after nuclear localization has been experimentally enforced. YFP–FADD–NLS expression constructs containing WT FADD or mutant FADD sequences linked to three simian virus 40 NLSs were transfected into MCF10a cells. Attached or (15 min) detached cells treated in the presence or absence of a Fas-agonistic antibody (2R2) were then scored for nuclear (N) or nuclear plus cytoplasmic (N + C) localization of the fluorescent tag; representative images used to score the cells are shown (*Top*), and quantitation of the results is shown in the histogram (*Middle*). The percentages of NC cells under attached conditions (without 2R2) were on average 2% greater for YFP–FADD–NLS than for YFP–NLS. [A, YFP–NLS; B, YFP–FADD (WT)–NLS; C, YFP–FADD (S194A)–NLS; D, YFP–FADD (Δ1–80)–NLS.] (*Bottom*) Detachment of cells from matrix promotes the recruitment of endogenous FADD protein to cell surface Fas–FasL complexes. Cells were incubated with a Fas agonistic mAb (2R2) under attached (A) or suspended (S) conditions for the indicated times; complexes were immunoprecipitated and analyzed for FADD by Western blotting.

that conditions that sensitize the cell to FasL trigger a rapid export of some fraction of FADD from the nucleus. In either event, we suspected that FADD's nucleocytoplasmic transport was likely to be performed actively by a transport protein rather than occurring by diffusion. To investigate the transport mechanism, we noted that FADD is phosphorylated at Ser-194 (50, 51). The function of this phosphorylation is unknown; it is not, however, required for the interaction of FADD with caspase-8 or Fas (50).

When hemagglutinin (HA) epitope-tagged FADD was transfected transiently into MCF10a cells, most cells showed mainly nuclear staining. However, the mutation of Ser-194 to alanine caused the FADD to be almost uniformly distributed throughout the cell (Fig. 2*a*). Among other mutants tested, the only other alterations similarly affecting FADD localization were either the deletion of the death effector domain (DED) (amino acids 1–80) or point mutation of Phe-25 to a glycine, which disrupts DED homotypic interactions (52). Despite this finding, there was no obvious basic amino acid-containing NLS present in the region of Ser-194 or in the DED, suggesting an unusual import mechanism (discussed below).

We then established an assay for the nuclear export of FADD in which YFP-labeled FADD was forced to assume a nuclear localization at time 0, regardless of FADD mutations, caused by three simian virus 40 NLSs appended to the C terminus. This assay allowed us to assay mutants that were potentially defective in both import and export for export specifically. We found that a brief period of cell detachment from matrix caused the WT YFP–FADD–NLS to partially export from the nucleus, producing a nuclear-plus-cytoplasmic signal in ≈20–25% of the cells in 15 min, whereas the control YFP–NLS remained in 95% of the nuclei (Fig. 2*b*) This export may contribute to the increased FasL sensitivity of suspended compared with attached MCF10a cells (R.A.S. and S.M.F., unpublished work), which remains to be established. The export was not caused by anoikis-induced breakdown of the nuclear envelope, as evidenced by the aforementioned YFP-alone control, the fact that export preceded detectable caspase activation by several hours, and the insensitivity of export to the pan-caspase inhibitor zVAD-fmk (data not shown.) Moreover, the detachment of from matrix promoted the recruitment of endogenous FADD to cell-surface Fas–Fas antibody complexes (Fig. 2*b*), validating cell detachment as a stimulus for FADD export.

We used this assay to compare the export capabilities of various mutants of FADD. Interestingly, the S194A and DED mutations (that inhibited import) also inhibited export of FADD. Although the DED contained a leucine-rich sequence that was a potential signal for crm1-mediated export LTELKFLCL, mutations of the leucines in this sequence did not affect export; also, the crm1 inhibitor leptomycin B did not affect export of YFP–FADD–NLS at doses that completely prevented export of the crm1-cargo, protein kinase A-inhibitor (data not shown), suggesting that crm1 did not export FADD.

The observation that the same mutations prevented both FADD import and export and that a phosphorylation site was required for both suggested the involvement of a nucleocytoplasmic shuttle protein that interacted preferentially with phosphorylated cargoes. Such a protein has been identified recently in human cells: hmsn5/exportin-5 (53). Although this protein was originally dubbed an exportin, it was subsequently shown to act as an importin as well (54). FADD interacted efficiently with exportin-5/hmsn5 but not with crm1 in cotransfection experiments in 293T cells (Fig. 7, which is published as supporting information on the PNAS web site). Interestingly, the mutants of FADD that did not transport to or from the nucleus efficiently, S194A and Δ1–80, also did not interact efficiently with exportin-5/hmsn5. Furthermore, GST–FADD protein recovered from transfected 293T cells interacted *in vitro* with purified exportin-5/hmsn5 protein in the presence of activated Ran protein [in accordance with the role of activated Ran in nuclear transport by exportin-5 (53)]; however, the same FADD protein first subjected to dephosphorylation did not (Fig. 7). Taken together, exportin-5/hmsn5 is a candidate FADD-shuttling protein, which remains to be confirmed by protein ablation experiments (complicated by the fact that exportin-5 is required for viability). Nevertheless, the data clearly define a role for Ser-194 phosphorylation in determining the localization of FADD protein.

FADD Interacts with MBD4. We hypothesized that FADD may carry out a novel function in the nucleus. Thus, a cDNA library derived from MCF-7 mammary adenocarcinoma cells was screened for FADD-interacting proteins in a yeast two-hybrid system.

Surprisingly, about one-third of the positive clones were fragments of MBD4. MBD4's interaction with FADD was highly specific in yeast, as several unrelated bait proteins failed to interact with it (Fig. 8*a*, which is published as supporting information on the PNAS web site). Using MBD4 deletion mutants expressed in the yeast two-hybrid system, we mapped the interacting region of MBD4 to amino acids 400–455, which is immediately upstream of the glycosylase domain (Fig. 8*b*). The regions of FADD required for MBD4 interaction were mapped similarly, indicating that the DED (amino acids 1–80) was required for the interaction but the carboxyl-terminal tail region

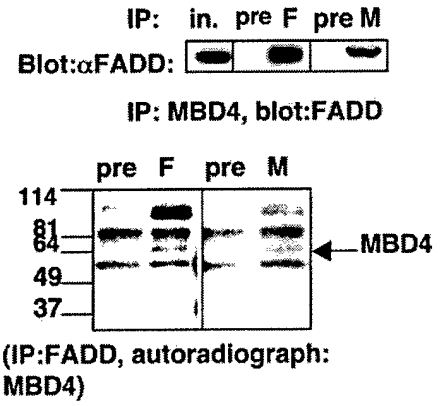

Fig. 3. FADD interacts with MBD4 in mammalian cells. (*Upper*) MCF10a lysates were immunoprecipitated (IP) with sheep anti-MBD4 antibody (M), anti-FADD polyclonal Ab (F), or preimmune serum (pre). Immunoprecipitates were analyzed by Western blotting using FADD mAb and a heavy v chain-specific anti-mouse secondary antibody. (*Lower*) Lysates from ^{32}P-labeled MCF10a cells were immunoprecipitated as above and the products were detected by autoradiography. Note that one of the two major antibody-specific bands precipitated with anti-FADD antibody comigrated with MBD4 (compare lanes M and F). The ≈90-kDa band precipitated with FADD antibody was suspected to be MLH1, which was confirmed below. All of the lanes shown were derived from the same gel; intervening lanes were deleted for clarity.

(needed for exportin-5 interaction as shown above) was not required (Fig. 8*c*). To test the sufficiency of the DED for MBD4 interaction, noting that the DED alone was not expressed well in yeast or 293T cells, the interaction was assayed *in vitro* by using recombinant proteins. Interestingly, the DED of FADD was reproducibly found to interact more efficiently with MBD4 than did full-length FADD (Fig. 8*c*). The involvement of the DED of FADD suggested that MBD4 and caspase-8 might compete against each other for binding to FADD, which was confirmed *in vitro* (data not shown).

To test the FADD–MBD4 interaction in mammalian cells, we first cotransfected epitope-tagged forms of the two proteins into 293T cells, pulling down one protein on glutathione beads and probing a Western blot for the other in both combinations (Fig. 9*a*, which is published as supporting information on the PNAS web site). FADD and MBD4 interacted efficiently and specifically by this criterion. We then assayed for the interaction of the endogenous proteins by coimmunoprecipitation (Fig. 3). A sheep polyclonal antibody was prepared against the C-terminal domain of bacterially expressed human MBD4 and its specificity was confirmed (Fig. 5*d*). This antibody was used to immunoprecipitate MBD4 from MCF10a lysates. These immunoprecipitates (in contrast to those with preimmune sheep IgG) contained a FADD signal that was readily detectable on Western blots with exposure times of <10 s. To perform the converse experiment (noting that the sheep anti-MBD4 did not work well for Western blot detection and that both FADD and MBD4 are phosphoproteins), cellular proteins were metabolically labeled with ^{32}P, and lysates were immunoprecipitated with our polyclonal FADD antiserum. The immunoprecipitates were analyzed by autoradiography of an SDS gel, revealing a specific band that precisely comigrated with MBD4 immunoprecipitated from parallel lysates, as well as a band of the molecular mass of MLH1 (≈87 kDa). Indeed, endogenous FADD immunoprecipitated from MCF10a cells revealed the presence of MLH1 protein by Western blot analysis (Fig. 9*b*), and 293T cotransfection confirmed that the DED was required for this association as well. These data indicate that endogenous FADD and MBD4 proteins interact in MCF10a cells.

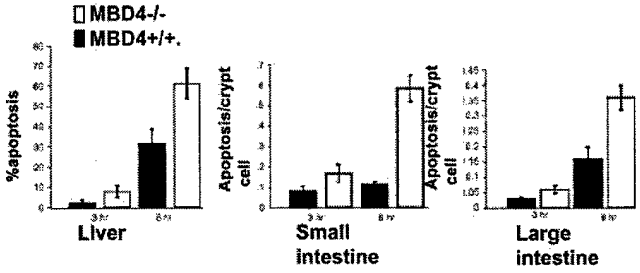

Fig. 4. MBD4 regulates FasL-induced apoptosis. MBD4 knockout or WT mice were injected with the agonistic Fas antibody Jo-2, and at the times indicated, intestinal crypt cells or hepatocytes were analyzed for apoptosis as described (47).

MBD4 Affects Apoptosis. The interaction of MBD4 with the caspase-8-activating protein FADD suggested that MBD4 might be capable of regulating apoptosis. To test this, we used our previously described MBD4 knockout mouse model (29). We recently observed evidence for a proapoptotic role of MBD4 with respect to DNA-damaging agents (O.J.S. and A.R.C., unpublished data). In light of the primary role of FADD in death receptor-induced apoptosis, WT control or MBD4 knockout mice were injected with the Fas-agonistic antibody Jo-2, which induces apoptosis rapidly in intestinal and hepatic epithelial cells that can be scored readily by histological analysis. Interestingly, the MBD4 knockout mice were reproducibly more sensitive (≈5.5-fold in the small intestine) to apoptosis in this context (Fig. 4). To examine the effect of MBD4 on FasL responses in MEFs, we rescued *MBD4*−/− MEFs with an HA–mouse–MBD4 retrovirus, generating mixed populations that expressed MBD4 at 3-fold above the WT MEF level (but substantially lower than the levels in established cell lines such as MCF10a; data not shown). This approach circumvented the comparison of cells from different embryos, which was confounded by variability. Surprisingly, MBD4 sensitized these cells, in contrast to the intestinal cells *in vivo*, to FasL-induced apoptosis (Fig. 10*a*, which is published as supporting information on the PNAS web site). This finding suggested that the effect of MBD4 on FasL-induced apoptosis depended on the cell type or the precise MBD4 expression level (which may in turn affect protein complex composition or MBD4 posttranslational modifications). Interestingly, MBD4 reexpression sensitized these MBD4-knockout cells to anoikis-related caspase activation as well (Fig. 10*b*).

Discussion

Nuclear Localization of FADD. FADD couples death receptors with initiator caspases (35–37). Thus, FADD is assumed to be primarily cytoplasmic. However, the evidence to support this assumption is limited to overexpressed FADD, which aggregates into "death effector filaments" (55, 56). These structures have not been observed for endogenous FADD, and, unlike endogenous FADD (R.A.S. and S.M.F., unpublished data) are Triton-insoluble (56). Thus, the localization of endogenous FADD protein was unexplored to our knowledge until the present report. The localization of FADD reported here does not imply that 100% of FADD is nuclear: clearly, the well-documented death receptor adaptor function of FADD logically implies that this is not the case. Thus, either there is a constitutive but minor cytoplasmic pool of FADD for this purpose or costimulatory signals for Fas signaling such as lack of cell-matrix adhesion (R.A.S. and S.M.F., unpublished data; refs. 43 and 44) stimulate the nuclear export of FADD. The latter is consistent with our results (Fig. 2*b*); thus, it will be interesting to determine how extracellular signals regulate FADD localization, as this could potentially modulate death ligand sensitivity. Control of Ser-194

phosphorylation, which is required for import/export and exportin-5 interaction, is likely to play a key role.

Significance of the FADD–MBD4 Interaction. MBD4 and FADD interacted with each other, suggesting a novel linkage between genome surveillance/DNA repair and apoptosis. Consistent with this finding, MBD4 was shown herein to control apoptosis. Preliminary data (not shown) using short-interfering RNA to reduce MBD4 protein levels in epithelial cell lines support this conclusion. The fact that MBD4 regulates FasL responses clearly implicates a functional connection between MBD4 and FADD, although more mechanistic information will be needed to conclude that MBD4 controls apoptosis by its direct FADD interaction.

Metazoan cells couple genome surveillance to apoptosis (reviewed in refs. 1, 12, and 57) to eliminate genetically aberrant and potentially neoplastic cells. We propose that MBD4-mediated genome surveillance is coupled directly to nuclear FADD, an adaptor protein implicated in multiple apoptotic responses (36–42). MBD4 is thought to specifically repair GT mismatches resulting from the spontaneous deamination of methylcytosine (25), the most frequent cause of point mutations in the human genome (28). In fact, MBD4 knockout mice show a mutator phenotype that leads to enhanced spontaneous carcinoma frequency in the *min* background (29). Thus, one compelling function for the MBD4–FADD complex would be to couple extensive "GT mismatch signals" to apoptosis.

The ability of MBD4 to regulate apoptotic responses to diverse DNA lesions (O.J.S. and A.R.C., unpublished data) or stimuli not apparently causing DNA damage is more challenging to explain. First, MBD4 interacts with MLH1 protein, and the latter promotes apoptosis triggered by a wide variety of DNA damage types (7–11), possibly because of its involvement in a large multifunctional DNA repair complex (58). Second, although FasL and anoikis are not considered DNA-damaging, they rapidly activate caspases, in turn activating nucleases that cause double-strand DNA breaks (59, 60). The latter would elicit DNA damage signals, thus activating caspases further in a feed-forward loop that finalizes the cell's commitment to apoptosis. The possible involvement of FADD and MBD4 in this amplification process, which would explain the proapoptotic effects of MBD4, remains to be determined.

In the context of intestinal crypt cells *in vivo*, MBD4 paradoxically suppressed FasL-induced apoptosis. Cell context-dependent effects of a gene knockout on apoptosis are not unprecedented (cf. ref. 61); this likely reflects cell-type differences in apoptotic signaling mechanisms. Conceivably, MBD4 sequesters FADD in the nucleus, thus inhibiting Fas function in this context. Alternatively, the relative concentrations of FADD, MBD4, and caspase-8 may be critical for the apoptotic output, because MBD4 at low concentrations promoted FADD–caspase-8 interaction but at high concentrations inhibited it *in vitro* (data not shown).

MBD4 is frequently mutated in human colorectal carcinoma cells, most commonly by frameshifts in the A10 repeat at position 301–310 (31–33), which would frameshift the downstream sequences including the glycosylase domain, MLH1 interaction domain, and FADD interaction domain. It will be of interest to mutationally inactivate each of these three functions independently to determine their contributions to apoptosis and understand whether this frameshift is potentially advantageous for tumor growth.

Finally, it has been reported that FADD is required for optimal cell cycle progression of activated T lymphocytes (62) and epithelial cells (R.A.S. and S.M.F., unpublished observations). When combined with the current observation that FADD is a component of a genome surveillance complex, one implication is that this complex may function in a cell cycle checkpoint with MLH1 or MBD4 to recognize the damage and FADD to arrest or promote progression through S phase.

We thank Ed Monosov and Souad Rahmouni for help with microscopy, Jean-Francois Cote and Miya Fujimoto for help with production of baculovirus proteins, Erica Golemis for advice and reagents for the yeast two-hybrid screens, Astar Winoto for the FADD-knockout MEFs, Ian Macara for a sample of exportin-5 protein, Carolyn Ho and Danielle Loughran for technical assistance, and Steve Linke and Robert Abraham for useful critique of the manuscript. The project was supported by National Institutes of Health Grant PO1 CA69381 (to S.M.F.), a Department of Defense Breast Cancer award (DAMD 17-00-0170) (to S.M.F.), a Canadian Institute of Health Research–Institut de Recherche Scientifique sur le Cancer Fellowship (to R.A.S.), and grants from Cancer Research U.K. (to A.R.C. and A.B.).

1. Abraham, R. T. (2001) *Genes Dev.* **15,** 2177–2196.
2. Wang, J. Y. (2000) *Oncogene* **19,** 5643–5650.
3. Khanna, K. K., Keating, K. E., Kozlov, S., Scott, S., Gatei, M., Hobson, K., Taya, Y., Gabrielli, B., Chan, D., Lees-Miller, S. P. & Lavin, M. F. (1998) *Nat. Genet.* **20,** 398–400.
4. Gong, J. G., Costanzo, A., Yang, H. Q., Melino, G., Kaelin, W. G., Jr., Levrero, M. & Wang, J. Y. (1999) *Nature* **399,** 806–809.
5. Kolodner, R. D. & Marsischky, G. T. (1999) *Curr. Opin. Genet. Dev.* **9,** 89–96.
6. Bellacosa, A. (2001) *J. Cell Physiol.* **187,** 137–144.
7. Hardman, R. A., Afshari, C. A. & Barrett, J. C. (2001) *Cancer Res.* **61,** 1392–1397.
8. Meyers, M., Wagner, M. W., Hwang, H. S., Kinsella, T. J. & Boothman, D. A. (2001) *Cancer Res.* **61,** 5193–5201.
9. Zhang, H., Richards, B., Wilson, T., Lloyd, M., Cranston, A., Thorburn, A., Fishel, R. & Meuth, M. (1999) *Cancer Res.* **59,** 3021–3027.
10. Humbert, O., Fiumicino, S., Aquilina, G., Branch, P., Oda, S., Zijno, A., Karran, P. & Bignami, M. (1999) *Carcinogenesis* **20,** 205–214.
11. Aebi, S., Fink, D., Gordon, R., Kim, H. K., Zheng, H., Fink, J. L. & Howell, S. B. (1997) *Clin. Cancer Res.* **3,** 1763–1767.
12. Bernstein, C., Bernstein, H., Payne, C. M. & Garewal, H. (2002) *Mutat. Res.* **511,** 145–178.
13. Formstecher, E., Ramos, J. W., Fauquet, M., Calderwood, D. A., Hsieh, J. C., Canton, B., Nguyen, X. T., Barnier, J. V., Camonis, J., Ginsberg, M. H. & Chneiweiss, H. (2001) *Dev. Cell* **1,** 239–250.
14. Roth, W., Stenner-Liewen, F., Pawlowski, K., Godzik, A. & Reed, J. C. (2002) *J. Biol. Chem.* **277,** 7501–7508.
15. Zhan, Y., Hegde, R., Srinivasula, S. M., Fernandes-Alnemri, T. & Alnemri, E. S. (2002) *Cell Death Differ.* **9,** 439–447.
16. Stegh, A. H., Schickling, O., Ehret, A., Scaffidi, C., Peterhansel, C., Hofmann, T. G., Grummt, I., Krammer, P. H. & Peter, M. E. (1998) *EMBO J.* **17,** 5974–5986.
17. Zheng, L., Schickling, O., Peter, M. E. & Lenardo, M. J. (2001) *J. Biol. Chem.* **276,** 31945–31952.
18. Doostzadeh-Cizeron, J., Yin, S. & Goodrich, D. W. (2000) *J. Biol. Chem.* **275,** 25336–25341.
19. Paroni, G., Henderson, C., Schneider, C. & Brancolini, C. (2002) *J. Biol. Chem.* **277,** 15147–15161.
20. Schickling, O., Stegh, A. H., Byrd, J. & Peter, M. E. (2001) *Cell Death Differ.* **8,** 1157–1168.
21. Torii, S., Egan, D. A., Evans, R. A. & Reed, J. C. (1999) *EMBO J.* **18,** 6037–6049.
22. Morgan, M., Thorburn, J., Pandolfi, P. P. & Thorburn, A. (2002) *J. Cell Biol.* **157,** 975–984.
23. Hendrich, B. & Bird, A. (1998) *Mol. Cell. Biol.* **18,** 6538–6547.
24. Bellacosa, A., Cicchillitti, L., Schepis, F., Riccio, A., Yeung, A. T., Matsumoto, Y., Golemis, E. A., Genuardi, M. & Neri, G. (1999) *Proc. Natl. Acad. Sci. USA* **96,** 3969–3974.
25. Hendrich, B., Hardeland, U., Ng, H. H., Jiricny, J. & Bird, A. (1999) *Nature* **401,** 301–304.
26. Petronzelli, F., Riccio, A., Markham, G. D., Seeholzer, S. H., Genuardi, M., Karbowski, M., Yeung, A. T., Matsumoto, Y. & Bellacosa, A. (2000) *J. Cell Physiol.* **185,** 473–480.
27. Petronzelli, F., Riccio, A., Markham, G. D., Seeholzer, S. H., Stoerker, J., Genuardi, M., Yeung, A. T., Matsumoto, Y. & Bellacosa, A. (2000) *J. Biol. Chem.* **275,** 32422–32429.
28. Krawczak, M., Ball, E. V. & Cooper, D. N. (1998) *Am. J. Hum. Genet.* **63,** 474–488.

29. Millar, C. B., Guy, J., Sansom, O. J., Selfridge, J., MacDougall, E., Hendrich, B., Keightley, P. D., Bishop, S. M., Clarke, A. R. & Bird, A. (2002) *Science* **297,** 403–405.
30. Boland, C. R. (2000) *Ann. N.Y. Acad. Sci.* **910,** 50–59; discussion 59–61.
31. Bader, S., Walker, M., Hendrich, B., Bird, A., Bird, C., Hooper, M. & Wyllie, A. (1999) *Oncogene* **18,** 8044–8047.
32. Bader, S., Walker, M. & Harrison, D. (2000) *Br. J. Cancer* **83,** 1646–1649.
33. Riccio, A., Aaltonen, L. A., Godwin, A. K., Loukola, A., Percesepe, A., Salovaara, R., Masciullo, V., Genuardi, M., Paravatou-Petsotas, M., Bassi, D. E., *et al.* (1999) *Nat. Genet.* **23,** 266–268.
34. Bellacosa, A. (2001) *Cell Death Differ.* **8,** 1076–1092.
35. Kischkel, F. C., Hellbardt, S., Behrmann, I., Germer, M., Pawlita, M., Krammer, P. H. & Peter, M. E. (1995) *EMBO J.* **14,** 5579–5588.
36. Chinnaiyan, A. M., O'Rourke, K., Tewari, M. & Dixit, V. M. (1995) *Cell* **81,** 505–512.
37. Boldin, M. P., Varfolomeev, E. E., Pancer, Z., Mett, I. L., Camonis, J. H. & Wallach, D. (1995) *J. Biol. Chem.* **270,** 7795–7798.
38. Micheau, O., Solary, E., Hammann, A. & Dimanche-Boitrel, M. T. (1999) *J. Biol. Chem.* **274,** 7987–7992.
39. Frisch, S. M. (1999) *Curr. Biol.* **9,** 1047–1049.
40. Rytomaa, M., Martins, L. M. & Downward, J. (1999) *Curr. Biol.* **9,** 1043–1046.
41. Shao, R. G., Cao, C. X., Nieves-Neira, W., Dimanche-Boitrel, M. T., Solary, E. & Pommier, Y. (2001) *Oncogene* **20,** 1852–1859.
42. Yuan, X. J. & Whang, Y. E. (2002) *Oncogene* **21,** 319–327.
43. Shain, K. H., Landowski, T. H. & Dalton, W. S. (2002) *J. Immunol.* **168,** 2544–2553.
44. Aoudjit, F. & Vuori, K. (2001) *J. Cell Biol.* **152,** 633–643.
45. Bhattacharya, D., Logue, E., Bakkour, S., DeGregori, J. & Sha, W. (2002) *Proc. Natl. Acad. Sci. USA* **99,** 8838–8843.
46. Toft, N. J., Winton, D. J., Kelly, J., Howard, L. A., Dekker, M., te Riele, H., Arends, M. J., Wyllie, A. H., Margison, G. P. & Clarke, A. R. (1999) *Proc. Natl. Acad. Sci. USA* **96,** 3911–3915.
47. Kuang, A. A., Diehl, G. E., Zhang, J. & Winoto, A. (2000) *J. Biol. Chem.* **275,** 25065–25068.
48. Gurney, T., Jr., & Foster, D. N. (1977) *Methods Cell Biol.* **16,** 45–68.
49. Gurney, T., Jr., & Collard, M. W. (1984) *Anal. Biochem.* **139,** 25–34.
50. Scaffidi, C., Volkland, J., Blomberg, I., Hoffmann, I., Krammer, P. H. & Peter, M. E. (2000) *J. Immunol.* **164,** 1236–1242.
51. Rochat-Steiner, V., Becker, K., Micheau, O., Schneider, P., Burns, K. & Tschopp, J. (2000) *J. Exp. Med.* **192,** 1165–1174.
52. Eberstadt, M., Huang, B., Chen, Z., Meadows, R. P., Ng, S. C., Zheng, L., Lenardo, M. J. & Fesik, S. W. (1998) *Nature* **392,** 941–945.
53. Brownawell, A. M. & Macara, I. G. (2002) *J. Cell Biol.* **156,** 53–64.
54. Yoshida, K. & Blobel, G. (2001) *J. Cell Biol.* **152,** 729–740.
55. Perez, D. & White, E. (1998) *J. Cell Biol.* **141,** 1255–1266.
56. Siegel, R. M., Martin, D. A., Zheng, L., Ng, S. Y., Bertin, J., Cohen, J. & Lenardo, M. J. (1998) *J. Cell Biol.* **141,** 1243–1253.
57. Wahl, G. M. & Carr, A. M. (2001) *Nat. Cell Biol.* **3,** E277–E286.
58. Wang, Y., Cortez, D., Yazdi, P., Neff, N., Elledge, S. J. & Qin, J. (2000) *Genes Dev.* **14,** 927–939.
59. Nagata, S. (2000) *Exp. Cell Res.* **256,** 12–18.
60. Kovacsovics, M., Martinon, F., Micheau, O., Bodmer, J. L., Hofmann, K. & Tschopp, J. (2002) *Curr. Biol.* **12,** 838–843.
61. Xu, Y. & Baltimore, D. (1996) *Genes Dev.* **10,** 2401–2410.
62. Zhang, J., Kabra, N. H., Cado, D., Kang, C. & Winoto, A. (2001) *J. Biol. Chem.* **276,** 29815–29818.

Fig. 5. Characterization of the antibodies used in this study. (a) Two of the FADD antibodies used in this study, the monoclonal from Transduction Laboratories (TL) and our polyclonal BUR385, were characterized by Western blotting of two-dimensional gels containing total MCF10a cell lysates. The two spots represent the unphosphorylated (more basic spot) and the phosphorylated (more acidic spot) forms of FADD seen in numerous previous publications on one-dimensional and two-dimensional gels (cf. ref. 1). Our second polyclonal anti-FADD, BUR386, was analyzed by standard Western blotting. (b) Our anti-mouse FADD antibody BUR404 was characterized by Western blotting of total cell lysates from FADD–/– MEFs vs. FADD-rescued MEFs. Note that, despite the presence of a weak background band on the blot, the FADD–/– MEFs showed no immunofluorescent signal above background with this antibody. (c) The MLH1 mAb from Oncogene Research was characterized by Western blotting lysates of an MLH1-deficient cell line, HCT116 (H),and an MLH1-expressing cell line LOVO (L). (d) Characterization of the sheep anti-MBD4 antibody (self-explanatory.)

1. Scaffidi, C., Volkland, J., Blomberg, I., Hoffmann, I., Krammer, P. H. & Peter, M. E. (2000) J. Immunol. 164, 1236–1242.

Fig. 6. FADD is mainly a nuclear protein. (a) Nuclear FADD staining is reduced by FADD short interfering RNA (siRNA) or genetic knockout of FADD. (Upper) MCF10a cells transfected with FADD siRNA or luciferase siRNA control were stained with FADD mAb. (Inset) A Western blot FADD levels (F, upper bands) and an actin control (A, lower bands) on proteins from luciferase (L) siRNA- or FADD (F) siRNA-treated cells. (Lower) A polyclonal antibody specific for mouse FADD was generated, shown to be specific by Western blotting, and used to stain FADD+/+ or FADD–/– MEFs. FADD fractionates as a nuclear protein. MCF10a cells lysed under hypotonic conditions were fractionated into "insoluble" (nuclei plus unbroken cells) and "soluble" fractions after low-speed centrifugation. A single Western blot was probed simultaneously with anti-caspase-3 antibody as a cytoplasmic marker protein and with anti-FADD antibody. Two representative experiments (out of three conducted) are shown. Intervening lanes were removed for clarity.

Fig. 7. Exportin-5/hmsn5 is a candidate nucleocytoplasmic transporter for FADD. (Upper) Interaction of FADD with hmsn5 but not crm1. (Left) GST-FADD expression constructs containing the FADD mutants indicated at the top were cotransfected with hmsn5-his expression constructs into 293T cells. Cell lysates were precipitated with glutathione-sepharose and the precipitates were analyzed on a Western blot by using anti-tetra-histidine antibody (top row.) The middle and bottom rows demonstrate the presence of the hmsn5-his and GST-FADD proteins in the transfected cell lysates. (Right) Gst-FADD or GST-PKI expression constructs were cotransfected with a crm1 expression construct into 293T cells and the glutathione-sepharose-precipitated protein was analyzed for crm1 on a Western blot (Upper); input gst proteins are shown (Lower). (Middle) Purified hsmn5 and FADD interaction is stimulated by activated Ran protein. Recombinant hmsn5-his protein (purified from Escherichia coli) was mixed with

recombinant GST-FADD (WT) or GST-FADD (S194A) protein (purified from transfected 293T cells) in the presence or absence of RanQ69L protein (purified from E. coli). After incubation, glutathione beads were washed and analyzed for hmsn5-FADD interaction by Western blotting with anti-tetra-his antibody. GST-p130cas was used as a negative control (ctrl). (Bottom) Phosphorylation of FADD is required for the FADD-hmsn5 interaction in vivo. GST-FADD was isolated from transiently transfected 293T cells and phosphatased while immobilized on glutathione beads with calf intestinal phosphatase (CIP) in the presence or absence of phosphatase inhibitors. After removal of the phosphatase, the eluted GST-FADD protein was allowed to interact with mbp-hmsn5 protein (isolated from transfected 293T cells on amylose resin). The top row shows the GST-FADD protein that interacted with MBP-hmsn5; the second and third rows show the input proteins.

Fig. 8. Identification of MBD4 as a candidate FADD interactor. (a) FADD-MBD4 interaction is specific in yeast. LexA-FADD (in pGilda) or lexA-control bait constructs were cotranformed into EGY48 yeast containing the lexA-lacZ reporter plasmid SH18-34 and an activation domain construct of MBD4 (MBD4/pJG4-5). Cotransformants were tested for lacZ activity by spotting colonies on 5-bromo-4-chloro-3-indolyl ?-D-galactoside plates, with the results shown in duplicate. Lane 1, lexA-FADD; lane 2, lexA-Ras(-CAAX); lane 3, lexA-KRIT(N-term); lane 4, lexA-KRIT(FERM); lane 5, lexA-HEF-1; lane 6, lexA-RBP7; lane 7, lexA-lamin; lane 8, lexA-CD40; lane 9, lexA-RFHM1; lane 10, lexA-FAS; lane 11, lexA-RBP4 cotransformed with its known interaction partner RBP7 (instead of MBD4). (b) FADD interacts with amino acids 400-455 of MBD4. For deletions without an asterisk, lexA-FADD was cotransformed with various deletion mutants of MBD4 as B42 activation domain fusions, and cotranformant colonies were assayed for lacZ activity. For deletions with an asterisk (*) lexA-MBD4 was cotransformed with B42-activation domain-FADD constructs. (c) MBD4 interacts with the death effector domain of FADD. (Upper) Various deletion mutants of FADD expressed as lexA fusions were cotransformed with the B42-MBD4(Cterm) fragment and cotransformants were assayed for lacZ activity. As the FADD DED alone could not be expressed in yeast (data not shown), in vitro interaction experiments using bacterially produced gst-FADD and baculovirus-produced his-MBD4 were performed (Lower) to show that the DED sufficed for MBD4 interaction. Gst, Gst-FADD (wt) or Gst-FADD (DED) proteins were used to pull down 6his-MBD4 protein, and the resulting pull-down blot is shown in the upper row, together with an amido black confirmation of input gst proteins.

Fig. 9. FADD interacts with MBD4 in mammalian cells. (a) FADD interacts with cotransfected MBD4. Gst-FADD (Upper) or Gst-MBD4 (Lower) were cotransfected with HA-MBD4 (Upper) or FADD-his (Lower). After precipitation of the lysates with glutathione beads, Western blots were probed with anti-HA or anti-6Xhis antibodies, respectively. Amido black-stained input proteins are shown. MLH1 is in a complex with FADD. (b) MLH1 is in a complex with FADD. (Upper) Endogenous FADD was immunoprecipitated from MCF10a lysates by using FADD pAb (F) or with preimmune

serum (pre). The immunoprecipitates were analyzed by Western blotting using an anti-MLH1 mAb. (Lower) The death effector domain (amino acids 1–80) of FADD is required for MLH1 association. 293T cells were cotransfected with the indicated HA-FADD constructs and FLAG-MLH1; the anti-HA immunoprecipitates were analyzed by Western blotting for FLAG-MLH1.

Fig. 10. MBD4 promotes FasL-induced apoptosis and anoikis in MEFs. (a) MEFs from MBD4-knockout embryos were rescued with mouse HA-MBD4 by using a retrovirus. The mixed, drug resistance-selected population, which was shown to be nearly 100% HA-MBD4 positive (+), or a mixed population of knockout cells infected with an empty retrovirus (-) were assayed for FasL-induced caspase activation. (b) MBD4 promotes anoikis in MEFs. Mixed populations of knockout or rescued cells as described in a were asayed for anoikis-related caspase activation after being held in suspension for the indicated times.

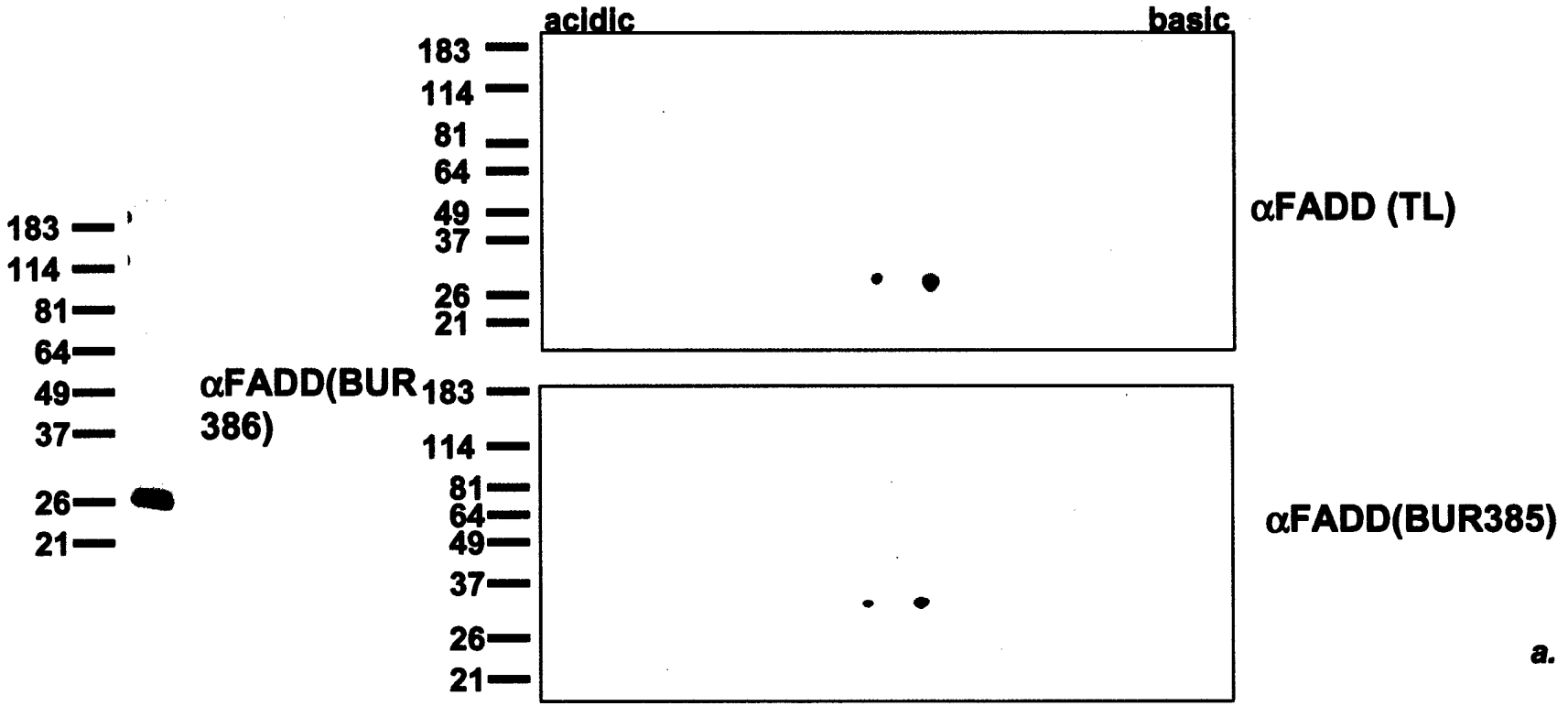
acidic
basic
183
114
81
64
49
37
26
21
αFADD (TL)
αFADD(BUR 386)
αFADD(BUR385)
a.

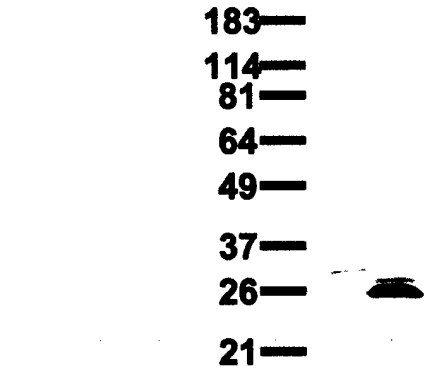
183
114
81
64
49
37
26
21
b.
FADD: -/- +/+

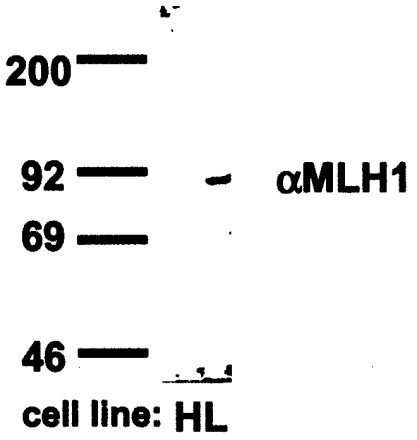
200
92
69
46
αMLH1
c.
cell line: HL

d. Characterization of sheep anti-MBD4 S157 (Data of Huck-Hui Ng and Adrian Bird)

Antigen: GST-hMBD4 aa371-580. This includes the glycosylase domain of MBD4.
Mouse and human MBD4 are 95.2% identical at the amino acid level over this region.

S157 anti-MBD4 antiserum

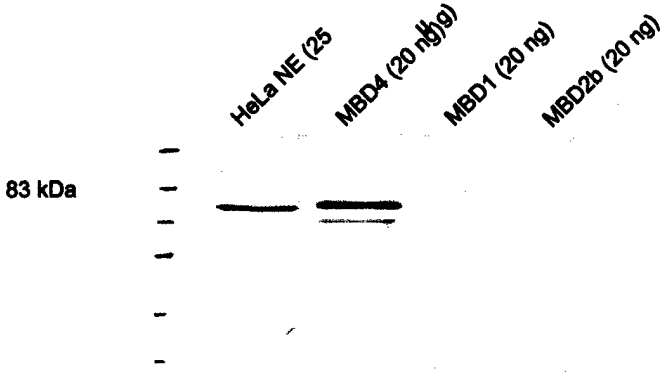

S157 detects endogenous human MBD4
In HeLa cell nuclear extracts, and also
recombinant MBD4, but does not cross
react with MBD1 or MBD2b

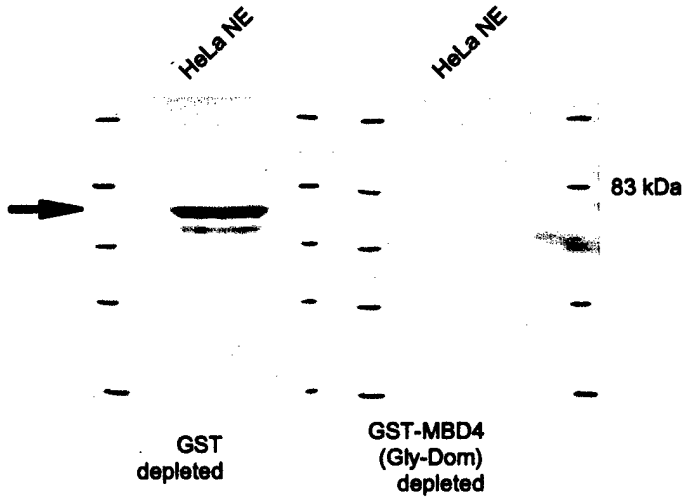

S157 depletes the 70kD band HeLa cell
nuclear extracts whereas antiGST antibodies do not.

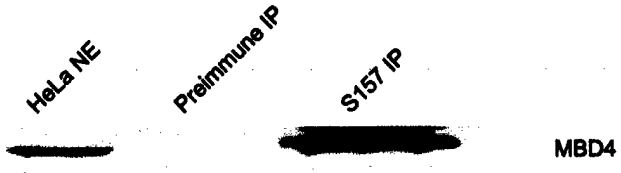

S157 immunoprecipitates from nuclear extracts
whereas preimmune serum does not.

a

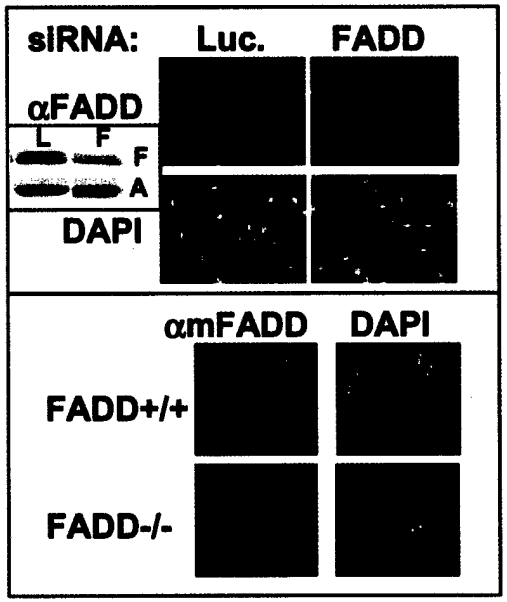
siRNA:
Luc.
FADD
αFADD
L
F
F
A
DAPI
αmFADD
DAPI
FADD+/+
FADD-/-

b

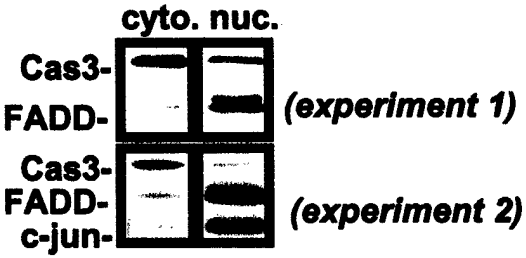
cyto. nuc.
Cas3-
FADD-
(experiment 1)
Cas3-
FADD-
c-jun-
(experiment 2)

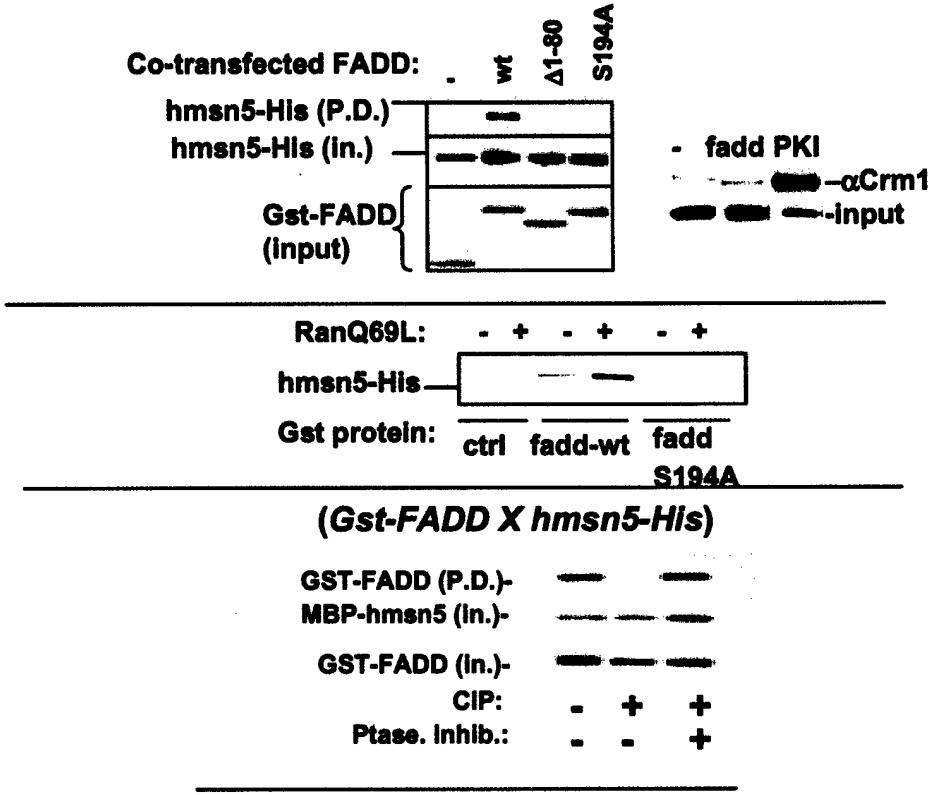
Co-transfected FADD:
-
wt
Δ1-80
S194A
hmsn5-His (P.D.)
hmsn5-His (in.)
Gst-FADD
(input)
- fadd PKI
αCrm1
input
RanQ69L:
- + - + - +
hmsn5-His
Gst protein:
ctrl
fadd-wt
fadd S194A
(Gst-FADD X hmsn5-His)
GST-FADD (P.D.)-
MBP-hmsn5 (in.)-
GST-FADD (in.)-
CIP:
- + +
Ptase. inhib.:
- - +

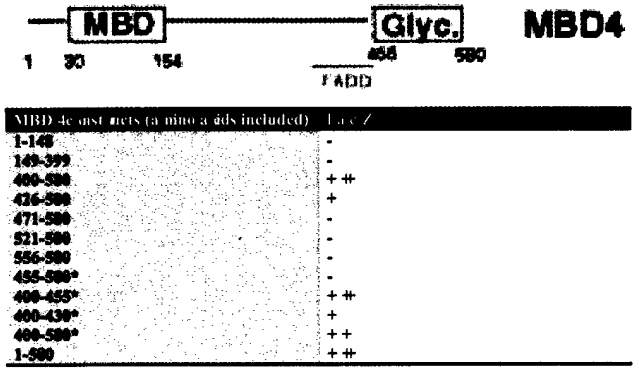

MBD4 constructs (amino acids included)	LacZ
1-148	-
149-399	-
400-580	++
426-580	+
471-580	-
521-580	-
556-580	-
455-580*	-
400-455*	++
400-430*	+
400-580*	++
1-580	++

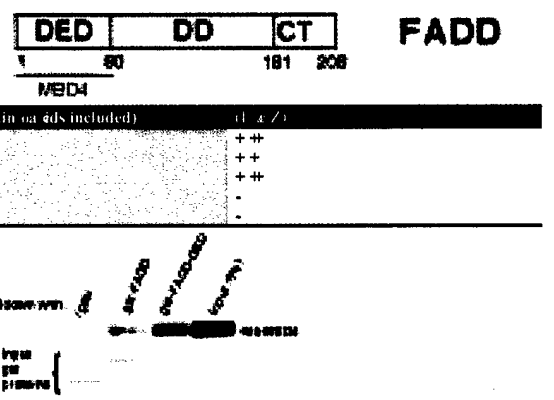

FADD Domains (amino acids included)	LacZ
1-208	++
1-192	++
1-183	++
81-208	-
181-208	-

a. ***b.*** ***c.***

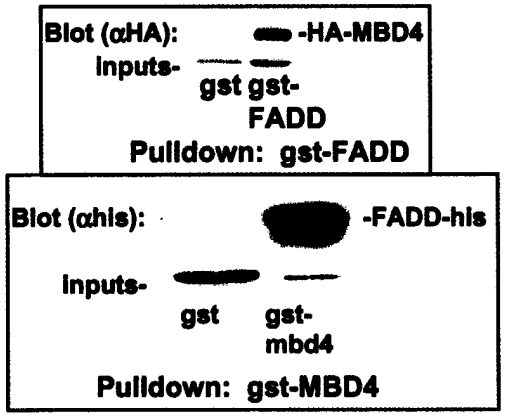
Blot (αHA):
-HA-MBD4
Inputs-
gst
gst-FADD
Pulldown: gst-FADD
Blot (αhis):
-FADD-his
Inputs-
gst
gst-mbd4
Pulldown: gst-MBD4

a.

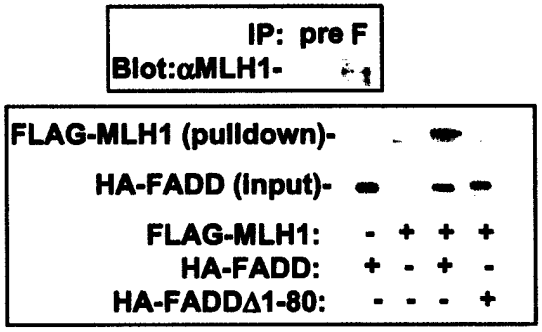
IP: pre F
Blot:αMLH1-
FLAG-MLH1 (pulldown)-
HA-FADD (input)-
FLAG-MLH1: - + + +
HA-FADD: + - + -
HA-FADDΔ1-80: - - - +

b.

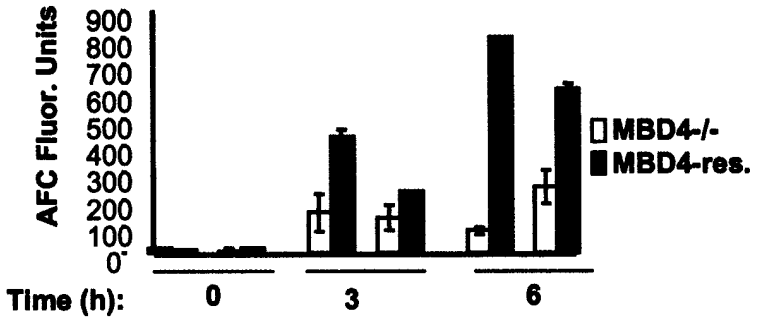
AFC Fluor. Units
900
800
700
600
500
400
300
200
100
0
MBD4-/-
MBD4-res.
Time (h):
0
3
6

a.

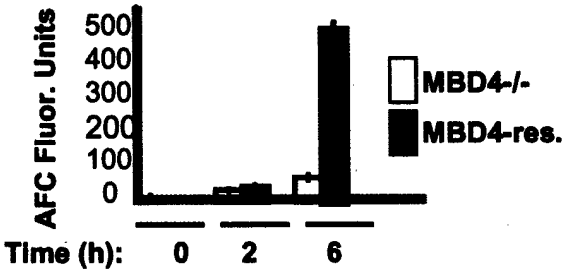
AFC Fluor. Units
500
400
300
200
100
0
MBD4-/-
MBD4-res.
Time (h):
0
2
6

b.